Chemistry & Biology
Article

Potent and Selective Peptidyl Boronic Acid Inhibitors of the Serine Protease Prostate-Specific Antigen

Aaron M. LeBeau,[1,2] Pratap Singh,[2,3] John T. Isaacs,[2,3] and Samuel R. Denmeade[1,2,3,*]
[1]Department of Pharmacology and Molecular Sciences
[2]The Sidney Kimmel Comprehensive Cancer Center at Johns Hopkins
[3]The Department of Chemical and Biomolecular Engineering
The Johns Hopkins University School of Medicine, Baltimore, MD 21231, USA
*Correspondence: denmesa@jhmi.edu
DOI 10.1016/j.chembiol.2008.05.020

SUMMARY

Prostate cancer cells produce high (microgram to milligram/milliliter) levels of the serine protease Prostate-Specific Antigen (PSA). PSA is enzymatically active in the extracellular fluid surrounding prostate cancers but is found at 1,000- to 10,000-fold lower concentrations in the circulation, where it is inactivated due to binding to abundant serum protease inhibitors. The exclusive presence of high levels of active PSA within prostate cancer sites makes PSA an attractive candidate for targeted imaging and therapeutics. A synthetic approach based on a peptide substrate identified first peptide aldehyde and then boronic acid inhibitors of PSA. The best of these had the sequence Cbz-Ser-Ser-Lys-Leu-(boro)Leu, with a K_i for PSA of 65 nM. The inhibitor had a 60-fold higher K_i for chymotrypsin. A validated model of PSA's catalytic site confirmed the critical interactions between the inhibitor and residues within the PSA enzyme.

INTRODUCTION

Prostate cancers selectively produce a number of unique prostate tissue differentiation markers. In particular, prostate cancer cells, like normal prostate epithelial cells, produce large amounts of Prostate-Specific Antigen (PSA) (Watt et al., 1986; Lilja et al., 2000). PSA is aptly named, in that it is specifically and exclusively produced by normal and malignant prostate epithelial cells and is not produced in any significant amounts by other normal tissue in the human male. On this basis, PSA is used extensively as a biomarker to screen for prostate cancer, to detect recurrence after local therapies, and to follow response to systemic therapies for metastatic disease (Watt et al., 1986; Lilja et al., 2000; Williams et al., 2007b; Denmeade and Isaacs, 2004).

However, accumulating evidence suggests that PSA may be more than just a biomarker and may play a role in the pathobiology of prostate cancer (Williams et al., 2007b). Functionally, PSA is a 33 kDa serine protease belonging to the human kallikrein gene family. In the freshly ejaculated semen, PSA maintains the semen in a semiliquid state through its ability to cleave the major gel-forming proteins semenogelin I (SgI) and semenogelin II (SgII), which are synthesized and secreted by the seminal vesicles (Malm et al., 2000; Lilja, 1985; Lilja et al., 1989). In normal prostate tissue, high concentrations of PSA are stored in the prostatic ductal network (Williams et al., 2007b). A very small quantity of enzymatically active PSA leaks out of the prostatic ductal network and forms complexes with the serum protease inhibitor α-1-antichymotrypsin (ACT) to generate the low nanogram/milliliter levels that can be measured in the circulation (Williams et al., 2007b).

In contrast, the disruption of normal tissue architecture in the prostate or distal sites by prostate cancer cells results in the leakage of increased amounts of PSA into the tissue interstitium and then into the circulation (Williams et al., 2007b). Enzymatically active PSA in the interstitium can subsequently degrade extracellular matrix proteins such as fibronectin and laminin. PSA can also release growth factors bound within the matrix structure. Previous in vitro studies have documented PSA's ability to cleave insulin-like growth factor binding protein 3 (IGFBP3) (Cohen et al., 1992), the small latent form of TGFβ2 (Dallas et al., 2005), and parathyroid-hormone-related protein (PTHrP) (Iwamura et al., 1996). More recent in vitro studies demonstrated that the PTHrP peptide fragment generated by PSA hydrolysis may function as an osteoblastic factor through activation of the endothelin A receptor (Schluter et al., 2001; Chirgwin et al., 2004).

Although these studies are compelling, it remains to be determined if these in vitro findings with purified proteins necessarily provide insights into whether PSA plays any relevant role in prostate cancer biology in vivo. The delineation of a functional role for PSA in the growth and progression of prostate cancer in vivo would be greatly facilitated by the availability of a small-molecule PSA inhibitor. To achieve this goal, in this study we describe the synthesis and characterization of potent and selective low-molecular weight, peptidyl-based PSA inhibitors. The template for the design of the inhibitor was a previously described PSA peptide substrate, identified from a map of cleavage sites within SgI and SgII (Denmeade et al., 1997). This substrate has been used to generate PSA-activated prodrugs and protoxins (Denmeade et al., 2003; Williams et al., 2007a). In the present study, we utilized an iterative approach toward developing peptidyl boronic acid-based PSA inhibitors with inhibition constant (K_i) values in

the low nanomolar range. A lead boronic acid-based inhibitor discovered by this method was found to be highly specific for PSA versus chymotrypsin and other serine and nonserine proteases. The inhibitor was further characterized for its ability to inhibit PSA degradation of PSA substrates and for its effects on PSA production and growth of PSA-producing xenografts in vivo.

RESULTS

Peptide Aldehyde Screening

PSA exhibits chymotrypsin-like activity, preferentially cleaving after hydrophobic residues such as leucine and tyrosine. This activity is due in part to the presence of a serine in the S-1 specificity pocket of the catalytic site. As a starting point for the synthesis of peptidyl boronic acid-based inhibitors of PSA, we chose to evaluate peptides based on a PSA substrate with the sequence Ser-Ser-Lys-Leu-Gln (SSKLQ) (Denmeade et al., 1997). Although previous studies in our laboratory demonstrated PSA's relatively unique ability to cleave peptide bonds after the amino acid glutamine (Denmeade et al., 1997), we opted to substitute the hydrophobic amino acids leucine and norleucine in the P1 position due to the complex nature of the glutamine side chain. Glutamine peptide aldehydes are severely limited in their utility since they exist mainly in the cyclic hemiaminal form (Webber et al., 1998), and the synthesis of a glutamine boronic acid is not feasible. Leucine and norleucine were selected because they were previously shown to be preferred P1 position substituents for PSA, and the synthesis of boronic acid derivatives of these two amino acids is known and can be accomplished in relatively high yield (Matteson et al., 1984, 1986).

Initially, we characterized inhibitors containing either the aldehyde Leu-H (i.e., SSKLL) or Nle-H (i.e., SSKLNle) in the P1 position (Table 1). From these studies, the calculated inhibition constants (K_i) were determined for Z-SSKLL-H and Z-SSKLNle-H to be 6.51 μM and 11.24 μM, respectively, for PSA. To confirm that the inhibition was not due merely to the occupancy of the catalytic site by the peptide, Z-SSKLL-OH and Z-SSKLNle-OH, as well as the corresponding amides of these peptides, were synthesized and tested (Table 1). Likewise, the peptide alcohol Z-SSKLL-CH_2OH did not inhibit PSA. Peptide versions of the PSA substrate used in the activity assay, without an AMC group at the C terminus, were also tested to rule out the possibility of product inhibition occurring during the duration of the assay. For all peptides lacking the C-terminal aldehyde functional group or aldehydes made from the D-isomer of both leucine and norleucine, the K_i values all were greater than 1000 μM. These studies document that the substitution of aldehyde-functionalized Leu or Nle in the P1 position of the PSA peptide substrate produces peptide aldehydes with K_i values in the low micromolar range.

Previously, a positional scanning approach was used to investigate amino acids preferred by PSA in each position (i.e., P1–P6) of a series of random peptides (Debela et al., 2006). This study documented that PSA has a preference for leucine in the P2 position (Debela et al., 2006). To evaluate whether peptides lacking a P2 leucine or other hydrophobic amino acids could still inhibit PSA, the aldehydes Z-SSKL-H and Z-SSKNle-H and the dipeptides Z-KL-H, Z-KNle-H, Z-QL-H, and Z-QNle-H (Table 1) were generated. All of the peptide aldehydes lacking a P2 hydrophobic amino acid had K_i values for PSA of > 1000 μM. In contrast, Z-LLL-H (MG132), a known 26S proteasome inhibitor, was synthesized and tested. Unlike the other inactive shorter peptide aldehydes, this peptide with P2 and P3 leucine residues had a K_i for PSA of 13.2 μM. Other amino acids were also evaluated in the P2 position of full-length sequences and included Z-SSKYL-H (K_i = 13.09 μM), Z-SSKQL-H (K_i = 21.8 μM), Z-SSKIL-H (K_i = 37.4 μM), Z-SSKKL-H (K_i = 57.8 μM), Z-SSKVL-H (K_i = 70.7 μM), and Z-SSKAL-H (K_i = 173.4 μM), as well as the dipeptide Z-YL-H (K_i = 541.4 μM) (Table 1). These results further document the preference for Leu in the P2 position.

In subsequent studies, we evaluated the contribution of amino acids in the P4-P5 position of the peptide (Table 1). The aldehyde lacking the P5 serine residue (Z-SKLL-H) had a ~6.5-fold higher K_i than the full-length sequence containing two serines. Peptide aldehydes lacking both P4 and P5 serine residues maintained

Table 1. K_i Values for PSA Inhibition by Leucine and Norleucine Aldehydes and Peptides

	Compound	K_i (μM)
	Leucine Aldehydes	
1	Z-SSKLL-H	6.51 ± 0.25
2	Z-SSKYL-H	13.09 ± 0.91
3	Z-SSKQL-H	21.79 ± 0.51
4	Z-SSKIL-H	37.43 ± 2.43
5	Z-SSKKL-H	57.85 ± 1.14
6	Z-SSKVL-H	70.71 ± 1.77
7	Z-SSKAL-H	173.4 ± 6.12
8	Z-SKLL-H	42.43 ± 2.13
9	Z-KLL-H	171.3 ± 6.88
10	Z-YL-H	514.4 ± 11.47
11	Z-KL-H	>1000
12	Z-QL-H	>1000
13	Z-SSKL-H	>1000
14	Z-SSKLL-H	>1000
15	Z-SSLKL-H	>500
16	Z-LKSSL	>1000
17	Z-LLL-H *(MG132)*	13.23 ± 0.86
	Norleucine Aldehydes	
18	Z-SSKLNle-H	11.24 ± 0.26
19	Z_KLNle-H	414.1 ± 22.49
20	Z-KNle-H	>1000
21	Z-QNle-H	>1000
22	Z-SSKNle-H	>1000
23	Z-SSKLNle-H	>1000
	Peptides	
24	Z-SSKLL-OH	>1000
25	Z-SSKLL-NH_2	>1000
26	Z-SSKLL-CH_2OH	>1000
27	Z-SSKLNle-OH	>1000
28	Z-SSKLNle-NH_2	>1000
29	Mu-SRKSQQY-OH	>1000
30	Mu-SRKSQQY-NH_2	>1000
31	Ac-HSSKLQL-OH	>1000

Table 2. K_i Values for PSA Inhibition by Leucine and Norleucine Boronic Acid Peptides

	Peptidyl Boronic Acid	K_i (μM)
32	Z-Q(boro)L	265.15 ± 18.39
33	Z-K(boro)L	353.5 ± 23.68
34	Z-SSK(boro)L	18.49 ± 1.48
35	Z-SSK(Boro)Nle	34.21 ± 0.83
36	Z-KL(boro)L	5.98 ± 0.24
37	Z-KL(boro)Nle	23.57 ± 0.47
38	Z-SSKL(boro)Nle	0.398 ± 0.020
39	Z-SSKL(boro)L	0.065 ± 0.005
	Derivatives with D-Isomer Amino Acids	
40	Z-SSKL(boro)L	0.149 ± 0.009
41	Z-SSKL(boro)L	21.48 ± 2.28
42	Z-SSKL(boro)L	28.67 ± 1.32
43	Z-SSKL(boro)L	75.76 ± 5.21
44	Z-SSKL(boro)L	32.21 ± 1.73
45	Z-SSKL(boro)L	227.27 ± 11.61
46	Z-SSKL(boro)L	439.94 ± 19.04
	Lysine Derivatives	
47	Z-SSL(boro)L	3.86 ± 0.29
48	Z-SSK(Ac)L(boro)L	0.294 ± 0.026

D-Amino acids are underlined.

the ability to inhibit PSA, but to a much lesser degree than the full-length sequences. Z-KLL-H and Z-KLNle-H had K_i values of 171.3 μM and 414.1 μM, respectively, which were 25- to 35-fold higher than the corresponding full-length inhibitors.

Peptidyl Boronic Acids

Peptide aldehydes have little utility in complex biological systems due to their inherent reactivity with numerous nucleophiles and cysteine proteases (Dufour et al., 1995). Although both aldehydes and boronic acids act as potent inhibitors of serine proteases by mimicking the tetrahedral transition state of peptide-bond hydrolysis (Thompson, 1973), boronic acids are more effective inhibitors (Walker and Lynas, 2001). Since our goal was to generate a PSA inhibitor that could be used in vivo, a strategy using peptidyl boronic acids was pursued by using the sequence preferences discovered in the primary peptide aldehyde screen.

In contrast to the results with the peptide aldehydes, the shorter dipeptidyl boronic acids Z-Q(boro)L and Z-K(boro)L now had measurable K_i values of 265 μM and 353 μM, respectively (Table 2). Even inhibitors lacking a P2 leucine exhibited a marked inhibitory improvement, with K_i values of Z-SSK(boro)L and Z-SSKL(boro)Nle now ranging from 18.49 μM to 34.21 μM. These values were both at least 50-fold lower than the K_i values for the corresponding aldehydes, which were both greater than 1000 μM (Table 2).

Significant improvement in the K_i was also observed for the P2 leucine-containing peptidyl boronic acids. The shortest P2 leucine inhibitors, Z-KL(boro)L and Z-KL(boro)Nle, both had low-micromolar K_i values of 5.98 μM and 23.57 μM, respectively. The K_i of Z-SSKL(boro)Nle was found to be submicromolar at 398 nM. However, the best PSA inhibitor that was developed by using this screening method was Z-SSKL(boro)L, which was found to have a K_i of 65 nM (Figure 1).

Z-SSKL(boro)L Sequence Modification

To further delineate the PSA pharmacophore and the relative importance of each amino acid residue to the inhibitory function of the Z-SSKL(boro)L inhibitor, D-amino acids were incorporated into each position of the sequence, except for the P1 boronic acid position, (Table 2). In positions P2–P4 of the peptide (i.e., **41**–**46**), incorporation of one or multiple D-amino acids markedly increased the K_i. In contrast, placing a D-serine in the P5 position of the inhibitor as in **40** did not completely abrogate function and only increased the K_i ~2-fold. These results further documented the relative importance of the P4 serine in comparison to the serine in the P5 position.

In additional studies, the contribution of the lysine in the P3 position of Z-SSKL(boro)L was addressed (Table 2). The presence of this lysine makes the inhibitor a potential substrate for degradation by trypsin-like proteases, thus possibly decreasing the half-life of the molecule in vivo. Z-SSL(boro)L, which lacks lysine in P3, still possessed some ability to inhibit PSA, with a K_i of 3.86 μM. Interestingly, the omission of lysine altogether produced a less dramatic effect than replacement with D-lysine, as evidenced by the ~8-fold higher K_i for Z-SSKL(boro)L compared to Z-SSL(boro)L. Substituting lysine with neutral N-ε-acetyl-lysine resulted in an inhibitor that was ~4.5-fold less potent, but still produced an inhibitor with a K_i below 300 nM.

Overall Binding Mode of Peptide Inhibitor

Previously, we described and validated a molecular model of the catalytic site for PSA (Singh et al., 2008). In order to gain insights into preferred binding interactions that might help in the design of additional PSA inhibitors, we used this model to study binding of the Z-SSKL(boro)L into the PSA catalytic site. Using this model, the overall binding orientation of peptide inhibitor ($S^5S^4K^3L^2$(boro)L^1) as produced by GOLD docking calculations is shown in Figure 1A. All residues except the P1 residue (L^1) are bound in an extended configuration, which is consistent with the canonical view of how peptide substrates and inhibitors bind at the catalytic pocket of serine proteases (Figure 2A). The backbone atoms of P3-P1 residues are in the correct orientation to form a short, antiparallel β sheet with residues 204–206 of PSA. This β sheet conformation is interrupted at the P1 residue, which adopts the values of dihedral angles in the right-handed α-helical (αR) region of the Ramachandran plot. The boronic moiety at the C terminus of the P1 residue is bound in a configuration mimicking the tetrahedral transition state during substrate hydrolysis (Figure 2B). The deprotonated oxygen of the boronic moiety makes a hydrogen bond with the protonated nitrogen (Nε2) of the catalytic triad His41 residue, whereas the hydroxyl group of the boronic moiety is oriented toward GLY 187 in the oxyanion hole. This orientation of the boronic moiety and the rest of the inhibitor is in agreement with the high-resolution crystal structure of serine proteases such as α-lytic protease crystallized with a transition state analog containing boronic acid (Bone et al., 1987).

Subsequently, we analyzed the side chain orientation of select amino acids residues in the P1-P5 position and determined the

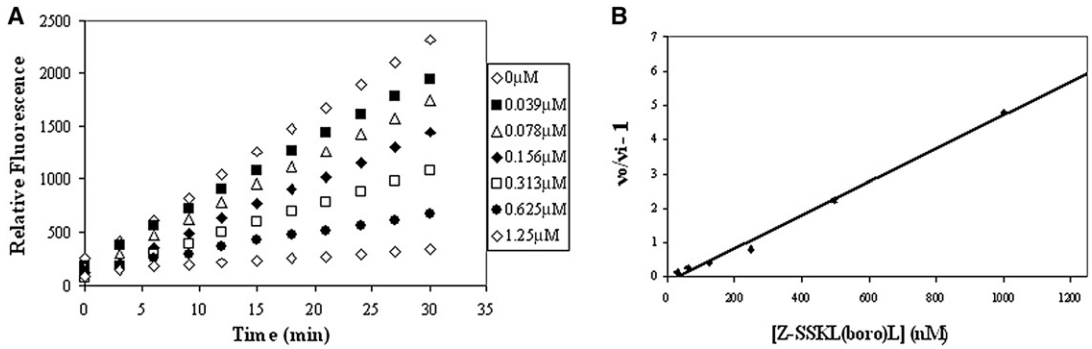

Figure 1. Experimental Methods by Which to Calculate K_i Values

(A) Example of progress curves for the inhibition of PSA by Z-SSKL(boro)L over a range of concentrations.

(B) Linear plot of $v_o/v_i - 1$ versus [I] for Z-SSKL(boro)L at indicated concentrations. The reciprocal of the slope of the line equals the apparent inhibition constant, $K_{i(app)}$. K_i is then calculated by using the equation $K_i = K_{i(app)}/(1 + [(S)/K_m])$. All assays were performed in triplicate; the average value at each time point was plotted.

nature of their energetic interactions with nearby protease residues (Figure 2B). The P1 residue (boroL1) binds at the specificity pocket lined by polar residues with the partial hydrophobic side chains such as S217, T184, and Y219. The presence of these residues imparts a hydrophobic character to the sides of the specificity pocket and, at the same time, a polar character to the bottom of the pocket. This allows for optimum binding of medium-sized hydrophobic residues such as leucine, but not of the large-sized residues such as tryptophan. These hydrogen bonds buried deep within the protease core are likely to be strong since the energetic penalty for an unsatisfied hydrogen bond buried in the protein core is very high. Our docking studies also suggested that although the unnatural amino acid norleucine binds at the P1 pocket in the correct conformation, the binding is energetically less favorable than the leucine residue. This finding is consistent with the observed K_i value of 398 nM for Z-SSKL(boro)Nle, which is ~5-fold higher than that of Z-SSKL(boro)L.

The model predicts that the P2 residue (L2) side chain is docked against the face of the imidazole ring of the catalytic His41 residue (Figure 2B). On the opposite side, the γ-branched side chain of leucine is in close contact with the hydrophobic Trp205 residue. Additionally, polar residues such as Ser93 and Tyr77 also line the farthest end of the P2 pocket, creating an electronegative potential and providing polar characteristics to the P2 pocket. Consistent with the mixed polar-hydrophobic characteristics of the P2 pocket, in silico positional scanning revealed that the P2 pocket is permissive in allowing residues ranging from polar ones such as tyrosine and hydrophobic residues such as leucine and norleucine. Exceptions are isoleucine (negative GOLD score), which sterically clashes with the P2 pocket residues. This finding correlates with the observed differences in the series of aldehyde inhibitors with different P2 residues, with only an ~2-fold higher K_i for Z-SSKYL-H but an ~6-fold higher K_i for Z-SSKIL-H compared to Z-SSKLL-H.

The P3 residue (K3) acts as a lid to the specificity pocket and docks at a location just above the P1-binding site in the specificity pocket. The aliphatic side chain of K3 is positioned in the vicinity of the hydrophobic phenylalanine group of the Phe141 residue and also in close contact with the methylene group of the Ser186 side chain (Figure 2B). More importantly, the free amine group of K3 is within 4.5 Å of the carboxyl moiety of the Glu208 side chain. Whereas the orientation of the Glu208 side chain is not ideal, there is a strong possibility for salt bridge formation with the ε-amine of K3. The presence of an acidic residue at position 208 is not common in the chymotrypsin family of serine proteases. The inhibitory potencies of modifications at the P3 position supported these insights. Modifications of the lysine residue that would potentially disrupt salt bridge formation with Glu208, such as acetylation of the lysine residue or elimination of the K3 residue, increase the K_i 5-fold and 60-fold, respectively.

The P4 pocket is located in the lower groove area and is mainly formed by His164, Pro165, Gln166, and Trp205 residues. The P4-binding pocket is bound by the kallikrein loop from above, but loop residues are not involved in any important energetic interactions. The Gln166 side chain is ideally placed to form a hydrogen bond with the hydroxyl of P4 serine (Figure 2B). The presence of Gln166 at this position is unique for PSA and not common in other serine proteases from the kallikrein family. The importance of this interaction with S4 is demonstrated by a marked increase in K_i for inhibitors lacking S4, with a 90-fold increase in K_i for Z-KL(boro)L and a 59-fold increase in K_i for Z-KL(boro)Nle. In addition, substitution of the D-isomer at the S4 position produces a 330-fold increase in the measured K_i. Finally, the S5 side chain is docked in the lower groove area, but it is exposed to the solvent, and there are no specific interactions with the protease residue. This suggests that P5 and additional N-terminal amino acid residues should not provide a significant contribution toward the overall binding affinity of the inhibitor molecule. This assertion is supported by our experimental finding that substitution of a D-isomer at S5 produced only a 2-fold increase in K_i (i.e., from 65 nM to 149 nM).

Specificity of the Z-SSKL(boro)L PSA Inhibitor

Having determined Z-SSKL(boro)L to be our best candidate inhibitor (K_i = 65 nM), we next determined its specificity for PSA relative to other proteases. The effect of Z-SSKL(boro)L as an inhibitor on the canonical serine proteases chymotrypsin and trypsin was investigated. Z-SSKL(boro)L was also tested with the serine proteases dipeptidyl peptidase 4 (DPP-4) and elastase and the nonserine proteases cathepsin B and cathepsin D, (Table 3). Although chymotrypsin is capable of cleaving after leucine residues, the K_i for inhibiting chymotrypsin was 60-fold

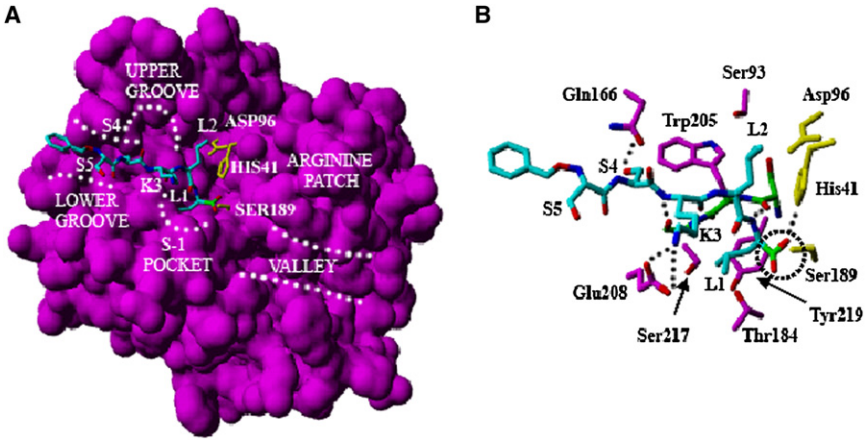

Figure 2. Binding Mode of Inhibitor Z-$S^5S^4K^3L^2$(boro)L^1 in the Catalytic Pocket of PSA

(A) Surface representation of a structural model of PSA and the overall orientation of the inhibitor in the catalytic site. Catalytic triad residues (HIS41, ASP96, and SER189) are shown in yellow. Also depicted are the major topological features of PSA structure, i.e., S-1 pocket, upper groove, lower groove, arginine patch, and valley region.

(B) Interactions of the Z-$S^5S^4K^3L^2$(boro)L^1 inhibitor with the key residues in the catalytic pocket. Catalytic triad residues are shown in yellow, the protease residues are shown in magenta, and the backbone of 204–206 residues is shown in green. Dotted lines represent hydrogen bonds, and the dotted circle pinpoints the exact location of the boronic acid moiety.

higher than for PSA. As was expected, the Z-SSKL(boro)L inhibitor did not inhibit trypsin or DPP-4 to any degree. Modest inhibition of elastase, another serine protease that prefers hydrophobic P1 residues, was observed. However, the inhibitor was still 22 times more selective for PSA over elastase. In an earlier study, we had demonstrated that the SSKLQ-AMC substrate could be hydrolyzed by the cysteine protease cathepsin B and the aspartyl protease cathepsin D (Denmeade et al., 1997). In contrast, no inhibition of either cathepsin B or cathepsin D by Z-SSKL(boro)L was observed over a range of concentrations, consistent with the fact that boronic acids alone are not effective inhibitors of cysteine or aspartyl proteases (Martichonok and Jones, 1997) . However, the lack of inhibition of these proteases by Z-SSKL(boro)L, even at high concentrations, demonstrates that the peptide sequence itself, although potentially a substrate for these proteases, is not capable of inhibiting the proteases in a noncovalent fashion.

Z-SSKL(boro)L Prevents the Degradation of Known PSA Substrates

In vitro PSA has been shown to cleave IGFBP3, resulting in the release of the prostatic mitogen IGF-1 (Cohen et al., 1992). In the bone, IGF-1 is known to be a strong promoter of osteoblastic activity (Chirgwin et al., 2004). Recombinant IGFBP3 was digested with PSA in the presence and absence of the inhibitor Z-SSKL(boro)L (Figure 3A). In the absence of the inhibitor, PSA completely degraded IGFBP3, as seen by the disappearance of the IGFBP3 band on the western blot. In contrast, the addition of the PSA inhibitor to the digest mixture protected IGFBP3 from degradation by PSA.

Previously, it was demonstrated in vitro that PTHrP 1–141, an endocrine hormone that stimulates bone resorption, can be hydrolyzed efficiently by PSA to release a 22 amino acid fragment (Iwamura et al., 1996). To study the effect an inhibitor could have on the PSA-mediated degradation of PTHrP, a 34 amino acid PTHrP peptide containg the PSA cleavage site was incubated with purified PSA (Figure 3B). After 1 hr, mass spectroscopic analysis demonstrated that PSA had completely digested the PTHrP peptide 1–34, cleaving the peptide after a Phe residue (RFF↓LHH). The resulting 22 amino acid fragment with an m/z of 2781.40 could be further cleaved, yielding a peptide with an m/z of 2193.06. PSA cleavage of the PTHrP peptide was completely inhibited in the presence of the inhibitor Z-SSKL(boro)L.

Table 3. Selectivity for PSA Inhibition by Z-SSKL(boro)L versus a Panel of Proteases

Protease	K_i (μM)	Selectivity[a]
PSA	0.065	1
Chymotrypsin	3.9	60
Trypsin	>100	>1500
DPPIV	>100	>1500
Cathepsin B	ND[b]	-
Cathepsin D	ND	-
Elastase	1.39	22

[a] Selectivity relative to PSA inhibition.
[b] ND, no detectable inhibition up to 500 μM.

Z-SSKL(boro)L Decreases the Clonal Survival of PSA-Producing Prostate Cancer Cells In Vitro

Previous in vitro studies have suggested a role for PSA in promoting the growth and invasion of human prostate cancer cells. To evaluate the effect of Z-SSKL(boro)L inhibition of PSA on growth, a panel of PSA-positive (LNCaP, LAPC-4, CWR22R, C4-2B) and negative (DU145, PC3) human prostate cancer cell lines was treated with the inhibitor at concentrations up to 15-fold higher than the K_i for PSA inhibition. In this study, cells were allowed to attach to the tissue culture plastic for 24 hr prior to exposure to the inhibitor. Under these conditions, the inhibitor at 100 nM showed a marginal effect and at 1 μM inhibited the growth of all cell lines, independent of PSA production, by 10%–25% (Figure 3C).

Besides the PSA substrates IGFBP3 and PTHrP described above, PSA has also been shown to be able to cleave extracellular matrix proteins such as fibronectin (Lilja et al., 2000) and release matrix-associated growth factors such as TGFβ (Dallas et al., 2005). These results suggest that PSA may possibly play a role in the process of extracellular matrix deposition required for cells to grow in vivo and to become established on plastic culture dishes in vitro. Therefore, in the next study, we assessed the ability of the Z-SSKL(boro)L inhibitor to inhibit attachment and subsequent clonal survival of newly plated individual cells. In this assay, the clonal survival of PSA-positive LNCaP human

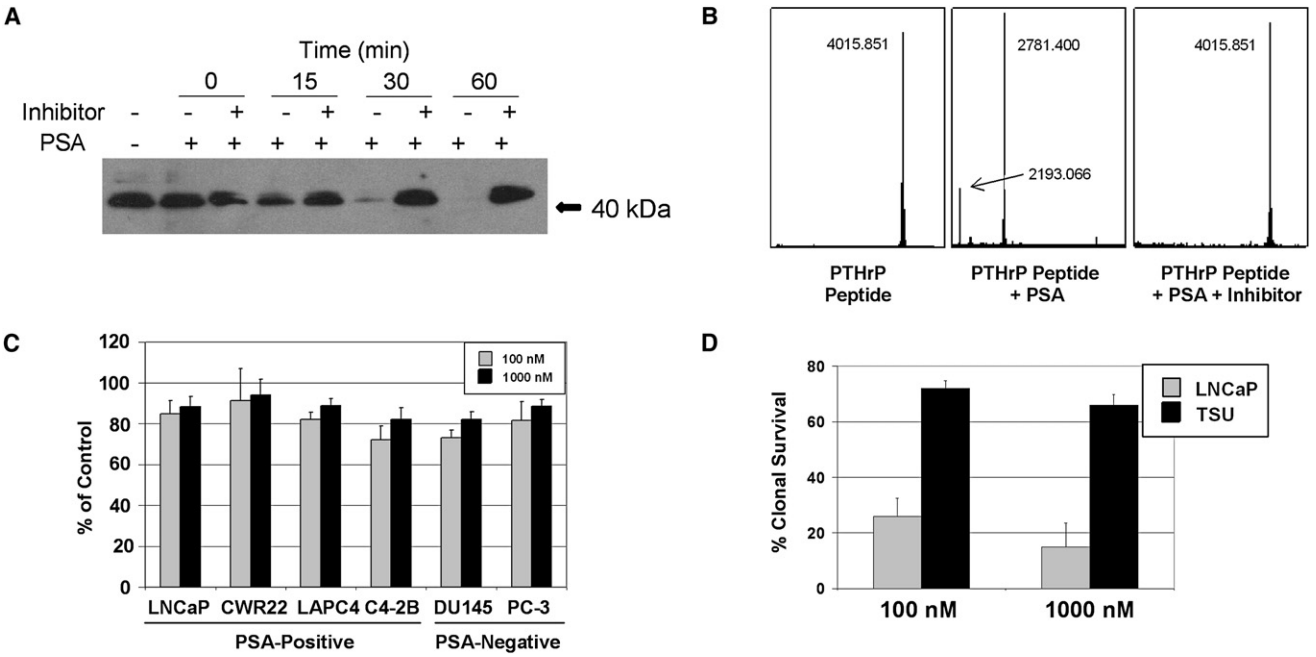

Figure 3. Z-SSKL(boro)L Inhibits the Degradation of PSA Substrates and the Clonal Survival of PSA-Producing Prostate Cancer Cells

(A) Western blot of IGFBP3 incubated with PSA ± the inhibitor Z-SSKL(boro)L.

(B) Digest of PTHrP peptide 1–34 with PSA ± the inhibitor Z-SSKL(boro)L. The digest was monitored by MALDI-TOF mass spectrometry.

(C) The effect of the inhibitor on the growth of indicated prostate cancer cell lines.

(D) The effect of the inhibitor on clonal survival of PSA-producing LNCaP cells and non-PSA-producing TSU human bladder cancer cells.

prostate cancer cells plated in the presence Z-SSKL(boro)L was inhibited ~75% at 100 nM and ~85% at 1 μM compared to vehicle-treated control (Figure 3D). In contrast, the clonal survival of PSA-negative TSU human bladder cancer cells was inhibited by only ~25% under these same conditions.

In Vivo Evaluation of the Lead PSA Inhibitor

On the basis of the in vitro results, the SSKL(boro)L inhibitor was subsequently evaluated in vivo for efficacy against CWR22R-H, a PSA-producing human prostate cancer xenograft. For in vivo studies, a more water-soluble form of the inhibitor was generated by substituting a morpholinocarbonyl (Mu) protecting group at the N terminus. This substitution did not affect the K_i for PSA inhibition (data not shown).

In initial toxicologic studies, it was determined that repeat intravenous doses of 33 mg/kg of the Mu-SSKL(boro)L inhibitor were well tolerated and had no significant effects on mouse body weight. A dose of 100 mg/kg produced transient weight loss, whereas a dose of 300 mg/kg was lethal to one-third of the mice. Therefore, the 33 mg/kg dose was used for subsequent in vivo studies. As control animals received equimolar doses of the inactive D-amino acid isomer **46** according to the same dosing schedule. The growth of tumors treated with these two peptidyl boronic acids was compared to vehicle-treated control (Figure 4A). The Mu-SSKL(boro)L inhibitor produced a slight decrease in tumor volume that only achieved statistical significance at day 6 prior to starting the second cycle of inhibitor (Figure 4A). The D-amino acid analog had no effect on tumor growth compared to control (data not shown).

However, whereas the inhibitor had minimal effect on growth, it had a relatively profound effect on measured PSA levels (Figure 4B). Free PSA levels were ~35% lower in the PSA inhibitor-treated animals, whereas total PSA (free PSA + complexed PSA) levels were ~30% lower (Figure 4B). No significant difference in PSA levels was observed for the inactive D-amino acid isomer-treated animals. Over the 10 day period between PSA measurements, the free PSA levels/gram of tumor increased by ~70% in the control animals, but only by 13% in the inhibitor-treated group (Figure 4C). Similarly, total PSA levels/gram of tumor increased 3.4-fold in the control-treated animals, but only 1.85-fold in the Mu-SSKL(boro)L-treated animals, whereas the D-amino acid analog had no significant effect on change in PSA compared to the control group.

DISCUSSION

The goal of this study was to develop a potent and selective peptide-based PSA inhibitor that could be used to help elucidate the role of PSA in the pathobiology of prostate cancer. These inhibitors potentially could be used for the development of prostate cancer-targeted therapies and imaging agents. Although an anti-PSA monoclonal antibody-based approach could also be envisioned, such a targeted antibody would have to be developed that could bind selectively to the high levels of enzymatically active PSA that are exclusively present in the extracellular peritumoral fluid within prostate cancer sites. This is an important caveat in the design of a PSA inhibitor given that multiple isoforms of PSA, all of which are enzymatically inactive, are present

A

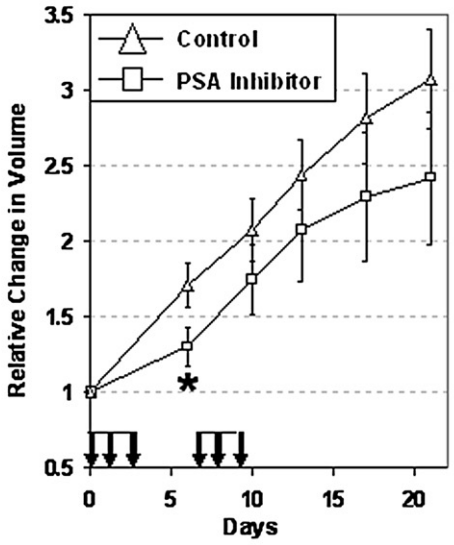

B

	PSA/g tumor (ng/ml/g)	
	Free PSA	Total PSA
Control	32.0 ± 3.8	328.7 ± 51.4
Inactive Inhibitor	27.6 ± 3.0	325.4 ± 32.7
PSA Inhibitor	21.3 ± 1.6	238.3 ± 20.3

C

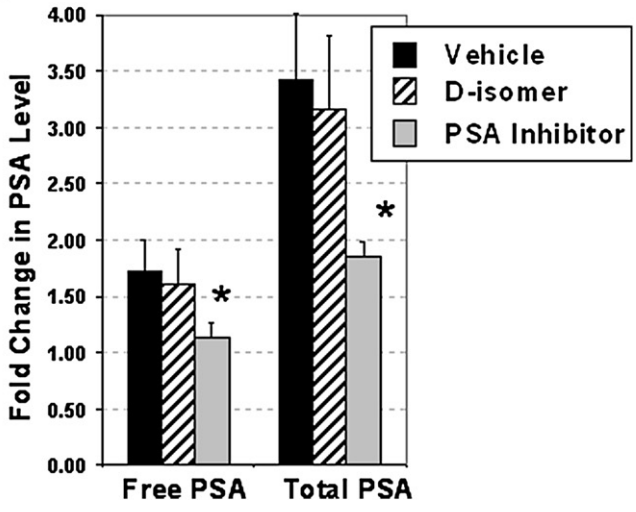

Figure 4. In Vivo Evaluation of Mu-SSKL(boro)L against Subcutaneous PSA-Producing CWR22R-H Xenografts

(A) Relative change in tumor volume of tumors in mice (n = 10/group) treated intravenously with either vehicle control or PSA inhibitor at a dose of 33 mg/kg/dose × 6 total doses. The days of dosing are indicated by arrows. The asterisk indicates $p < 0.05$ via a Student's t test.

(B) Serum levels of free and total PSA/gram of tumor measured 24 hr after the last dose of inhibitors. ($p < 0.05$ for both free PSA and total PSA levels in PSA inhibitor-treated animals versus vehicle controls).

(C) Fold change in free and total PSA/gram of tumor in mice treated with vehicle control or D-amino acid inhibitor or Mu-SSKL(boro)L at 33 mg/kg/dose × 6 doses. Fold increase is equal to (1 − [ratio of PSA/gram of tumor measured 24 hr after the sixth dose of inhibitor compared to PSA/gram of tumor measured 24 hr prior to the first dose of inhibitor]). The asterisk indicates $p < 0.05$ via a Student's t test.

in the circulation of patients with prostate cancer. Therefore, an advantage of this peptide-based inhibitor approach is that it selectively targets the proteolytic activity of PSA present only in the extracellular fluid of prostate cancers. Peptides have a number of additional distinct advantages over antibody-based approaches (Bander, 2006). These include small size, easy preparation, toleration of the harsh conditions of chemical modifications or radiolabeling, higher penetration into tumors, low toxicity, and potential high affinity and specificity for the protease catalytic site. On this basis, a number of peptide-based approaches for imaging and therapy are currently in use clinically (Okarvi, 2004; Sato et al., 2006; Kane et al., 2003), including bortezomib, a peptidyl boronic acid-based proteasome inhibitor approved for the treatment of multiple myeloma.

For in vivo studies, both the potency and selectivity of the PSA inhibitor are of paramount importance in the selection of a "lead" inhibitor candidate. In these studies, we determined that the Z-SSKL(boro)L inhibitor had a K_i of ~65 nM, making this compound the most potent PSA inhibitor described to date. In addition, our overall design strategy produced inhibitors that were relatively selective for PSA inhibition. From the outset, the mechanisms underlying boronic acid-based protease inhibition limited the inhibitory potential only to the serine/threonine protease class. The inclusion of a hydrophobic amino acid in the P1 position adds further specificity by preventing nonspecific inhibition of trypsin and trypsin-like serine proteases (Martichonok and Jones, 1997).

To evaluate the unique interactions between the amino acids in the Z-SSKL(boro)L inhibitor and residues within the PSA catalytic site., we used a molecular model of the PSA catalytic site that was developed based on the crystal structure of porcine kallikrein and HK1, two proteins with relatively high sequence homology to PSA. In particular, HK1 has it kallikrein loop in the correct orientation and provides an ideal template on which to build a PSA homology model. This model was previously validated by using a series of published β-lactam compounds (Singh et al., 2008; Adlington et al., 2001). Subsequent to these studies, the crystal structure of PSA bound to an anti-PSA antibody was published (Ménez et al., 2008). However, we have assessed the goodness of the fit between our homology model and the crystal structure and found that the root means square difference (rmsd) value for all atoms is 2.2 Å, indicating that the homology model is indeed structurally very similar to the published crystal structure. Furthermore, structurally important residues in the catalytic pocket have the same conformation in both structures, further justifying the high confidence and validity of our homology model.

PSA does share some substrate preferences with chymotrypsin, such as hydrophobic residues like leucine in the P1 position. Thus, the selectivity of the PSA inhibitor for inhibition of PSA versus chymotrypsin appeared to be due to unique binding interactions between the side chains of the additional amino acids in the Z-SSKL(boro)L inhibitor and residues within the PSA catalytic site. These modeling studies demonstrated a potential for salt

bridge formation between the P3 Lys and Glu208 and a hydrogen bond between the hydroxyl of P4 serine and the side chain Gln166 in the PSA protein. Chymotrypsin lacks such an acidic residue at position 208, and the presence of Gln166 at this position is unique for PSA and not common in other serine proteases. These observations may in part explain the observed 60-fold difference in K_i values for PSA and chymotrypsin even though leucine was placed in the P1 position.

In vivo, the lead PSA inhibitor was marginally active against a subcutaneous PSA-producing human prostate cancer xenograft. These results suggest that the PSA inhibitor may not be adequately inhibiting PSA production within the xenograft. Alternatively, PSA activity may play no functional role in the growth of this subcutaneously implanted xenograft. Existing data support a role for PSA in the generation of osteoblastic bone metastases. The ability of our inhibitor to block the degradation of PTHrP and cleavage of IGFBP3 suggests that our inhibitor may produce a more significant biologic response in a more relevant model. This question is being addressed in ongoing studies in our laboratory by using intratibial prostate tumor implantation as a model for osteoblastic metastases. Regardless of the model, future in vivo mechanistic studies with the PSA inhibitor will require further optimization of the in vivo stability and pharmacokinetics of the peptidyl-based inhibitor.

Although the inhibitor did not significantly inhibit the growth of the PSA-producing xenografts, the effect of the inhibitor on serum PSA levels provides evidence of a biological effect. Although tumor sizes of the control- and PSA inhibitor-treated groups were relatively equal at the time of PSA measurement, the inhibitor-treated animals had significantly lower levels of both free and total PSA compared to both vehicle-treated controls and animals treated with the D-amino acid isomer, which was a very poor inhibitor of PSA in vitro. These results suggest that the PSA inhibitor may be altering the clearance of PSA from the circulation. Enzymatically active PSA that is released into the circulation forms a complex with either α-1-antichymotrypsin (ACT) or α-2-macroglobulin (A2M) (Williams et al., 2007b). PSA rapidly forms an irreversible complex with A2M that is rapidly cleared by the liver (i.e., $t_{1/2}$ = minutes). The magnitude of the PSA-A2M complex formation in men with prostate cancer is unknown, as this PSA form cannot be measured via ELISA-based assays. In contrast, the kinetics of PSA-ACT complex formation is slow, and the half-life of the complex is hours to days. PSA-ACT can be measured via ELISA and is the major form of PSA in the circulation. Our working hypothesis is that the PSA inhibitor may alter PSA binding to ACT, thereby increasing irreversible entrapment by A2M in the serum. The end result of this increased clearance is an overall decrease in measurable PSA levels in the circulation. Further studies are ongoing in support of this hypothesis.

SIGNIFICANCE

Large amounts of enzymatically active PSA are continuously produced by all stages of prostate cancer, including cancers in men with advanced, high-grade, hormone-refractory cancer. This observation, coupled with growing experimental evidence, suggests that PSA plays an important role in the pathobiology of prostate cancer. These observations also support the development of PSA-selective inhibitors as useful tools to further validate PSA as a therapeutic target. In addition, the exclusive production of active PSA only in the tumor interstitium with subsequent rapid inhibition by serum protease inhibitors emphasizes that PSA is truly a "prostate-specific" protein that has yet to be exploited therapeutically or as an imaging target. The significance of this work, therefore, is that we describe a rational and iterative approach to develop potent and highly selective PSA inhibitors based on previously known PSA peptide substrate. As we describe, the PSA peptide inhibitor discovered by this approach is a useful tool that can be used to evaluate the role of PSA in the growth, invasion, and metastasis of prostate cancer. The modeling studies provide insights as to additional modifications that could be made to optimize the peptide for in vivo applications. The chemical flexibility of the peptide platform allows for easy modification of the peptide. The modeling studies and the recently published crystal structure document that bulky moieties such as cytotoxin and imaging agents could be added to the amino terminus of the peptide inhibitor without interfering with its ability to inhibit PSA. Future studies with these inhibitors will be directed toward developing a fuller understanding of the role of PSA in prostate cancer development and progression and the generation of PSA-targeted therapies and imaging agents.

EXPERIMENTAL PROCEDURES

Peptide Aldehyde and Boronic Acid Synthesis

For synthetic details, see the Supplemental Data (available online).

PSA Assays and Inhibition Kinetics

The assay for PSA activity was performed as previously described (Denmeade et al., 1997). The PSA concentration per assay was 2.5 μg/ml (2 nM active PSA) with a PSA substrate concentration of 300 μM. Substrate hydrolysis ± inhibitor over a range of concentrations was monitored by measuring fluorescence change secondary to AMC release by using a Fluoroskan 96-well fluorometric plate reader (excitation, 355 nm; emission, 460 nm) connected to a Macintosh computer with Deltasoft 3 software. Complete hydrolysis of the substrate was maintained below 5% to ensure that the substrate concentration was essentially constant. K_i values were determined by using the method of progress curves as described earlier (Salvesen and Nagase, 2001). Data were plotted as $v_o/v_i - 1$ versus [I], where v_o is the rate of substrate hydrolysis in the absence of inhibitor, v_i is the rate of substrate hydrolysis in the presence of inhibitor, and [I] is the concentration of PSA inhibitor. The plots of $v_o/v_i - 1$ versus [I] were linear, with the reciprocal of the slope of the line equal to the apparent inhibition constant, $K_{i(app)}$. The inhibition constant, K_i, was then calculated by using the equation $K_i = K_{i(app)}/(1 + [(S)/K_m])$. The K_m value of the PSA substrate, Mu-SRKSQQY-AMC (California Peptides), was 140 μM, as determined by kinetic analysis with Sigma Plot software.

Homology Model of PSA

The three-dimensional structural model of PSA was developed based on the crystal structure of porcine kallikrein (PDB code: 2PKA) and the human tissue kallikrein HK1 (PDB code: 1SPJ). The details of the model construction and the software package used for model building are described in a previous study that reported the application of this model for gaining mechanistic insights into the inhibition of PSA by the β-lactam class of molecules (Singh et al., 2008). This homology model of PSA has its kallikrein loop in a semi-open configuration, which results in a catalytic site accessible to both inhibitors and substrates. This model is an improvement over previous models of PSA that were developed by using a single template and a de novo kallikrein loop design (Coombs et al., 1998; Villoutreix et al., 1994), which is less accurate than the loop design based on actual crystal structure templates, such as the human tissue kallikrein structure (1SPJ) used in our study.

GOLD Docking Protocols

For our docking studies, the GOLD v3.0 program developed by CCDC (Cambridge, UK) was used to dock peptide inhibitors into the catalytic site of PSA by using previously described methods (Singh et al., 2008). The catalytic site was defined by a spherical space with 25 Å radius centered on the catalytic serine residue (Ser189). For every peptide inhibitor, 20 independent runs (GA = 20) were performed, resulting in 20 different docking poses ranked by their GOLD Score. For every independent run, the number of operations performed (Nop) was 100,000. To eliminate personal bias, the top-scoring pose for every peptide inhibitor was used as the most probable binding conformation. To guide the docking process, a single distant constraint was used, which restrained the boron atom of the C-terminal boronic acid moiety within 1.5–3.5 Å from the side chain oxygen atom of catalytic serine residue (Ser189) by using a spring constant of 5 kcal/mol.

Ligand preparation for the docking studies was done by using the MOE software package (CCG, Montreal). All peptidic inhibitors were built in an extended conformation by using the Builder module within the software package, and partial charges were assigned by using the CHARM22 force field. Special attention was paid while building the boronic moiety at the end of the C terminus of the peptide inhibitors since this part of the molecule forms transition state-like tetrahedral interactions with the catalytic serine side chain and the ε nitrogen (Nε2) of the catalytic histidine residue (His41).

PSA Inhibitor Specificity Studies

The inhibitory constants for each protease tested were determined by using the method mentioned previously. For determining the inhibitor specificity for cathepsin D, a Cathepsin D Assay Kit (Sigma) was used according to the manufacturer's specifications with the substrate Mca-GKPILFFRLK-Dnp. The conditions for other protease assays were: DPP-4 (5 nM) + 400 μM AP-AFC in a buffer of 100 mM Tris and 100 mM NaCl (pH 7.8); cathepsin B (7 nM) + 50 μM Z-RR-AMC in a buffer of 50 mM acetate, 2.5 mM DTT, and 2.5 mM EDTA (pH. 5.5); elastase (1.5 nM) + 20 μM suc-AAPV-AMC; trypsin (5 nM) + 200 μM Bz-R-AMC; chymotrypsin (2 nM) + 25 μM suc-AAF-AMC. These three proteases were assayed by using 50 mM Tris and 0.1 M NaCl (pH 7.8).

PTHrP Peptide Digest with PSA

PTHrP peptide 1–34 (1.0 μM) was digested with 2 nM PSA in PSA assay buffer ± inhibitor (1.5 μM) at 37°C for 1 hr. Aliquots of the digests were taken at different time points, desalted by using P10-C_{18} ZipTips (Millipore), and spotted (0.5 μl) on a MALDI-TOF plate. Spots were mixed with 0.5 μl matrix consisting of 10 mg/ml recrystalized cyano-4-hydroxy cinnamic acid in 50% ethanol/water. Mass spectra were acquired on an Applied Biosystems Voyager DE-STR MALDI-TOF mass spectrometer at the Johns Hopkins School of Medicine Mass Spectrometry and Proteomics Facility. The mass spectrometer was calibrated by using the ProteoMass Peptide MALDI Calbration Kit (Sigma). All spectra were acquired in positive ion mode.

IGFBP3 Digest with PSA

IGFBP3 (500 ng) was incubated with purified PSA (50 ng) ± 500 nM inhibitor in PSA assay buffer at 37°C. Aliquots were taken at different time points, and the digests were quenched by freezing in liquid nitrogen. Digests were resolved on Bio-Rad Ready Gels, 4%–15% Tris-HCl. IGFBP3 was visualized by using a purified goat polyclonal antibody raised against the C terminus of IGFBP3 (Santa Cruz Biotechnology).

Cytotoxicity Assays

Assays were performed by using the PSA-producing cell line LNCaP (human prostate cancer), and non-PSA producing TSU (human bladder cancer) was purchased from ATCC and maintained in RPMI-1640 supplemented with 10% fetal bovine serum at 37°C, 5% CO_2, humidified air as previously described (Christensson et al., 1990). After cells were exposed to agent for 72 hr, MTT cell proliferation assays were performed according to the manufacturer's instruction, and clonal survival assays were performed as previously described (Christensson et al., 1990).

In Vivo Studies

In vivo studies were performed by using the PSA-producing human prostate cancer xenograft CWR22R-H. This model is passaged as a xenograft and grows in a castrated host. Derivation and characterization of this xenograft has been previously described (Chandran et al., 2007). Animals bearing subcutaneous CWR22R-H xenografts (n = 10 per group) received intravenous injection of test compounds in sterile normal saline. Tumors were measured by using vernier calipers, and tumor volume was determined by using the formula L × W × H × 0.5236. Body weight was measured twice weekly. All animal studies were performed according to procedures and protocols approved by the Johns Hopkins University Animal Care and Use Committee.

SUPPLEMENTAL DATA

Supplemental Data include the synthetic protocols and characterization data for all of the peptide aldehyde and boronic acid compounds described in this report and are available at http://www.chembiol.com/cgi/content/full/15/7/665/DC1/.

ACKNOWLEDGMENTS

We greatly appreciate the advice on chemical syntheses provided by Aneta Modzelewska and Surojit Sir at Johns Hopkins. This work was supported by an award from the One-in Six Foundation, Akron, Ohio.

Received: February 18, 2008
Revised: May 9, 2008
Accepted: May 28, 2008
Published: July 18, 2008

REFERENCES

Adlington, R.M., Baldwin, J.E., Becker, G.W., Chen, B., Cheng, L., Cooper, S.L., Hermann, R.B., Howe, T.J., McCoull, W., McNulty, A.M., et al. (2001). Design, synthesis, and proposed active site binding analysis of monocyclic 2-azetidinone inhibitors of prostate specific antigen. J. Med. Chem. *44*, 1491–1508.

Bander, N.H. (2006). Technological insight: monoclonal anti-body imaging of prostate cancer. Nat. Clin. Pract. Urol. *3*, 216–225.

Bone, R., Shenvi, A.B., Kettner, C.A., and Agard, D.A. (1987). Serine protease mechanism: structure of an inhibitory complex of α-lytic protease and a tightly bound peptide boronic acid. Biochemistry *26*, 7609–7614.

Chandran, S.S., Nan, A., Rosen, D.M., Ghandehari, H., and Denmeade, S.R. (2007). A prostate-specific antigen activated N-(2-hydroxypropyl) methacrylamide copolymer prodrug as dual-targeted therapy for prostate cancer. Mol. Cancer Ther. *6*, 2928–2937.

Chirgwin, J.M., Mohammad, K.S., and Guise, T.A. (2004). Tumor-bone cellular interactions in skeletal metastases. J. Musculoskelet. Neuronal Interact. *4*, 308–318.

Christensson, A., Laurell, C.-B., and Lilja, H. (1990). Enzymatic activity of prostate-specific antigen and its reactions with extracellular serine proteinase inhibitors. Eur. J. Biochem. *194*, 755–765.

Cohen, P., Graves, H.C., Peehl, D.M., Kamarei, M., Giudice, L.C., and Rosenfeld, R.G. (1992). Prostate-specific antigen (PSA) is an insulin-like growth factor binding protein-3 protease found in seminal plasma. J. Clin. Endocrinol. Metab. *75*, 1046–1053.

Coombs, G.S., Bergstrom, R.C., Pellequer, J.L., Baker, S.I., Navre, M., Smith, M.M., Tainer, J.A., Madison, E.L., and Corey, D.R. (1998). Substrate specificity of Prostate- Specific Antigen (PSA). Chem. Biol. *5*, 475–488.

Dallas, S.L., Zhao, S., Cramer, S.D., Chen, Z., Peehl, D.M., and Bonewald, L.F. (2005). Preferential production of latent transforming growth factor b-2 by primary prostatic epithelial cells and its activation by prostate-specific antigen. J. Cell. Physiol. *202*, 361–370.

Debela, M., Magdolen, V., Schechter, N., Valachova, M., Lottspeich, F., Craik, C.S., Choe, Y., Bode, W., and Goettig, P. (2006). Specificty profiling of seven human tissue kallikreins reveals individual subsite preferences. J. Biol. Chem. *281*, 25678–25688.

Denmeade, S.R., and Isaacs, J.T. (2004). The role of prostate-specific antigen in the clinical evaluation of prostatic disease. BJU Int. *93* (*Suppl 1*), 10–15.

Denmeade, S.R., Lou, W., Lövgren, J., Malm, J., Lilja, H., and Isaacs, J.T. (1997). Specific and efficient peptide substrates for assaying the proteolytic activity of Prostate-specific Antigen. Cancer Res. *57*, 4924–4930.

Denmeade, S.R., Jakobsen, C., Janssen, S., Khan, S.R., Lilja, H., Christensen, S.B., and Isaacs, J.T. (2003). Prostate-specific antigen-activated thapsigargin prodrug as targeted therapy for prostate cancer. J. Natl. Cancer Inst. *95*, 990–1000.

Dufour, E., Storer, A.C., and Menard, E. (1995). Peptide aldehydes and nitriles as transition state analog inhibitors of cysteine proteases. Biochemistry *28*, 9136–9143.

Iwamura, M., Hellman, J., Cockett, A.T., Lilja, H., and Gershagen, S. (1996). Alteration of the hormonal bioactivity of parathyroid hormone-related protein (PTHrP) as a result of limited proteolysis by prostate-specific antigen. Urology *48*, 317–325.

Kane, R.C., Bross, P.F., Farrell, A.T., and Pazdur, R. (2003). Velcade®: U.S. FDA approval for the treatment of multiple myeloma progressing on prior therapy. Oncologist *8*, 508–513.

Lilja, H. (1985). A kallikrein-like serine protease in prostatic fluid cleaves the predominant seminal vesicle protein. J. Clin. Invest. *76*, 1899–1903.

Lilja, H., Abrahamsson, P.-A., and Lundwall, A. (1989). Semenogelin, the predominant protein in human semen. Primary structure and identification of closely related proteins in the male accessory sex glands and on the spermatozoa. J. Biol. Chem. *264*, 1894–1900.

Lilja, H., Piironen, T.P., Rittenhouse, H.G., Mikolajczyk, S.D., and Slawin, K.M. (2000). Comprehensive Textbook of Genitourinary Oncology (Philadelphia, PA: Lippincott Williams and Wilkins Publishers).

Malm, J., Hellman, J., Hogg, P., and Lilja, H. (2000). Enzymatic action of prostate-specific antigen (PSA or hK3) substrate specificity and regulation by $Zn^{(2+)}$, a tight-binding inhibitor. Prostate *45*, 132–139.

Martichonok, V., and Jones, J.B. (1997). Cysteine proteases such as papain are not inhibited by substrate analogue peptidyl boronic acids. Bioorg. Med. Chem. *5*, 679–684.

Matteson, D.S., Jesthi, P.K., and Sadhu, K.M. (1984). Synthesis and properties of pinanediol α-amido boronic esters. Organometallics *3*, 1284–1288.

Matteson, D.S., Sadhu, K.M., and Peterson, M.L. (1986). 99% chirally selective synthesis via pinanediol boronic esters: insect pheromones, diols, and an amino alcohol. J. Am. Chem. Soc. *108*, 810–819.

Ménez, R., Michel, S., Muller, B.H., Bossus, M., Ducancel, F., Jolivet-Reynaud, C., and Stura, E.A. (2008). Crystal structure of a ternary complex between human prostate-specific antigen, its substrate acyl intermediate and an activating antibody. J. Mol. Biol. *376*, 1021–1033.

Okarvi, S.M. (2004). Peptide-based radiopharmaceuticals: future tools for diagnostic imaging of cancers and other diseases. Med. Res. Rev. *24*, 357–397.

Salvesen, G.S., and Nagase, N. (2001). Finding, purification, and characterization of natural protease inhibitors. In Proteolytic Enzymes, Second Edition, R. Benyon and J.S. Bond, eds. (Oxford: Oxford University Press), pp. 131–147.

Sato, A.K., Viswanathan, M., Kent, R.B., and Wood, C.R. (2006). Therapeutic peptides: technological advances driving peptides into development. Curr. Opin. Biotechnol. *17*, 638–642.

Schluter, K.D., Katzer, C., and Piper, H.M. (2001). A N-terminal PTHrP peptide fragment void of a PTH/PTHrP-receptor binding domain activates cardiac ETA receptors. Br. J. Pharmacol. *132*, 427–432.

Singh, P., Williams, S.A., Shah, M.H., Lectka, T., Pritchard, G.J., Isaacs, J.T., and Denmeade, S.R. (2008). Mechanistic insights into the inhibition of prostate specific antigen by β-lactam class compounds. Proteins *70*, 1416–1428.

Thompson, R.C. (1973). Use of peptide aldehydes to generate transition-state analogs of elastase. Biochemistry *12*, 46–51.

Villoutreix, B.O., Getzoff, E.D., and Griffin, J.H. (1994). A structural model for the prostate disease marker, human prostate-specific antigen. Protein Sci. *3*, 2033–2044.

Walker, B., and Lynas, J.F. (2001). Strategies for the inhibition of serine proteases. Cell. Mol. Life Sci. *58*, 596–624.

Watt, K.W.K., Lee, P.-J., M'Timkulu, T., Chan, W.-P., and Loor, R. (1986). Human Prostate-Specific Antigen: structural and functional similarity with serine proteases. Proc. Natl. Acad. Sci. USA *83*, 3166–3170.

Webber, S.E., Okano, K., Little, T.L., Reich, S.H., Xin, Y., Fuhrman, S.A., Matthews, D.A., Love, R.A., Hendrickson, T.F., Patick, A.K., et al. (1998). Tripeptide aldehyde inhibitors of human rhinovirus 3C protease: design, synthesis, biological evaluation and cocrystal structure solution of P1 glutamine isosteric replacements. J. Med. Chem. *41*, 2786–2805.

Williams, S.A., Merchant, R.F., Garrett-Mayer, E., Isaacs, J.T., Buckley, J.T., and Denmeade, S.R. (2007a). A prostate-specific antigen-activated channel-forming toxin as therapy for prostatic disease. J. Natl. Cancer Inst. *99*, 376–385.

Williams, S.A., Singh, P., Isaacs, J.T., and Denmeade, S.R. (2007b). Does PSA play a role as a promoting agent during the initiation and/or progression of prostate cancer? Prostate *67*, 312–329.